Journal of Food Engineering 234 (2018) 73–81

Contents lists available at ScienceDirect

Journal of Food Engineering

journal homepage: www.elsevier.com/locate/jfoodeng

Mathematical modeling of L-(+)-ascorbic acid delivery from pectin films (packaging) to agar hydrogels (food)

Gianluca Chiarappa [a], Maria D. De'Nobili [b], Ana M. Rojas [b], Michela Abrami [a], Romano Lapasin [a], Gabriele Grassi [c], José A. Ferreira [d], Elias Gudiño [e], Paula de Oliveira [d], Mario Grassi [a, *]

[a] Department of Engineering and Architecture, University of Trieste, Via A. Valerio 6, 34127 Trieste, Italy
[b] Departamento de Industrias, Facultad de Ciencias Exactas y Naturales, University of Buenos Aires, Ciudad Universitaria, 1428 Buenos Aires, Argentina
[c] Department of Life Sciences, Cattinara University Hospital, Trieste University, Strada di Fiume 447, I-34149 Trieste, Italy
[d] CMUC, Department of Mathematics of University of Coimbra, 3001-454 Coimbra, Portugal
[e] Department of Mathematics, Federal University of Paraná, Curitiba, Brazil

ARTICLE INFO

Article history:
Available online 13 April 2018

Keywords:
Mathematical modeling
Packaging
Ascorbic acid
Pectin edible films
Agar hydrogels

ABSTRACT

This paper focusses on the mathematical modeling of the ascorbic acid (antioxidant) release from a pectin edible film (packaging) to an agar hydrogel (food). The proposed model considers the viscoelastic properties of the polymeric film, the solid ascorbic acid dissolution inside the film, its degradation and diffusion in both the film and the hydrogel. By relying on the independent determination of all its parameters, the model proved to predict the ascorbic acid transport inside the agar hydrogel properly. Thus, it may be considered a powerful theoretical tool for the design of polymeric films (packaging) aimed at releasing antioxidant agents inside food.

1. Introduction

Edible films and coatings are promising systems for improving food quality, shelf life, safety, and functionality. They are able to incorporate additives such as anti-browning agents, antimicrobials, flavors, colorants, and other functional substances (Martín-Belloso et al., 2009) possible including in the future nucleic acid based drugs (Grassi and Marini, 1996; Grassi et al., 2010; Grassi et al., 2004). Antioxidants are employed to prevent oxidative rancidity, degradation, and enzymatic browning in fruits and vegetables. L-(+)-ascorbic acid (AA) is a reducing agent and also a water-soluble antioxidant for food preservation. In recent years, there has been an increasing demand for natural antioxidants, chiefly because of the negative toxicological reports on many synthetic compounds (Miková, 2001). The importance of antioxidants is well recognized in food preservation and the supply of essential substances in vivo (Shi, 2001). Several authors have explored the possibility of incorporating anti-browning agents like AA into edible films used to coat minimally processed fruits (Wong et al., 1994; Baldwin et al., 1996; Lee et al., 2003; Perez-Gago et al., 2006). Rojas-Graü et al. (2007) and Tapia et al. (2005) applied alginate- and gellan-based coatings over fresh-cut apples and papayas thus demonstrating that coatings are suitable carriers for antioxidant agents, including cysteine, glutathione, and ascorbic and citric acids.

In previous works, low-methoxyl pectin (LMP) based films were successfully developed to support and stabilize AA in view of its antioxidant protection at food interface (De'Nobili et al., 2011). Pectins are complex polysaccharides present in the primary cell walls of plants. They are rich in galacturonic acid and often contain significant amounts of rhamnose, arabinose, and galactose as well as thirteen other different monosaccharides (Vincken et al., 2003). Three major pectic polysaccharides are known: homogalacturonan (HG), rhamnogalacturonan-I (RG-I), and rhamnogalacturonan-II (RG-II) (Pérez et al., 2000; Willats et al., 2006). Commercial pectins, however, are primarily composed of HG because the lateral substitution of the RG-I kinks is partially hydrolyzed during the extractive process (Voragen et al., 2009). As other biopolymers, pectins are able to form continuous crystalline and/or amorphous microstructures like films. Thus, pectin films containing AA have a strong possibility of extending food shelf life or increasing the safety of foods as packaging or coating materials.

With the aim of reducing the total amount of preservatives

* Corresponding author.
E-mail address: mario.grassi@dia.units.it (M. Grassi).

https://doi.org/10.1016/j.jfoodeng.2018.04.011
0260-8774/

added to food, the edible coating or film may be designed to contain active ingredients ensuring a highly effective antioxidant action at food surface where oxidative reactions usually occur. Accordingly, a deep knowledge of film mass transport properties represents a decisive factor in the development of antioxidant food packaging systems. This, in turn, implies a clear understanding of the macro- and microscopic properties of the film/food couple (Grassi et al., 2007). In this frame, in a previous work of ours, the macro- and nanoscopic characteristics of edible pectin films and agar cylinders, mimicking foods, were determined by means of rheology and low-field nuclear magnetic resonance (LF-NMR). The aim of this paper is, therefore, to describe, according to a mathematical modeling approach, the antioxidant (AA) transport from a packaging film (LMP) to food, here represented by an agar hydrogel. As the antioxidant containing film was placed in contact with food in a dry state, two mass balances must be considered. The first one is related to the AA movement from the film to food, while the second one considers the water leaving food and swelling the film. In particular, the second mass balance assumes that the water presence causes an internal stress field, described by the generalized Maxwell's model, depending on the viscoelastic nature of the film. The principal advantage of this strategy consists in the possibility of embodying the film viscoelastic properties directly in the two mass balances.

2. Mathematical model

The physical reference for our model is depicted in Fig. 1, where the spatial disposition and the characteristic lengths of the LMP film and the agar hydrogel are displayed. The water molecules, moving from the agar hydrogel to the initially dry LMP film, are responsible for the film swelling, which, in turn, promotes the AA dissolution and diffusion toward the agar hydrogel. In the attempt to simplify the entire scenario to be modeled, three major hypotheses were formulated. The first one concerns the possibility of reducing the intrinsically three-dimensional transport problem to a simpler one-dimensional system in the light of the experimental setup depicted in Fig. 1. Thus, it is implicitly assumed that, except the contact surface, the LMP film and agar surfaces are perfectly impermeable to water and AA. While the impermeability to AA is quite obvious (in the experimental conditions, AA vapor pressure is negligible), in order to prevent a water loss, the system constituted by the agar hydrogel and the LMP film was placed into a sealed and thermostated environment containing a water-soaked gauze which ensures the water saturation in the vapor phase. The second hypothesis regards the ideal behavior of the polymers-water-AA system so that all possible mixing effects may be neglected. Finally, the third hypothesis assumes no direct effect (a sort of drag effect) on the mass transport deriving from the water and AA molecules movement in the opposite direction. As commonly supposed (Grassi et al., 2007), it is assumed that the AA and water motions are unable to affect reciprocally, even if water could indirectly affect AA transport, thus allowing AA dissolution (from a solid state to a dissolved one) and enhancing its diffusivity due to the enlargement of the LMP film meshes.

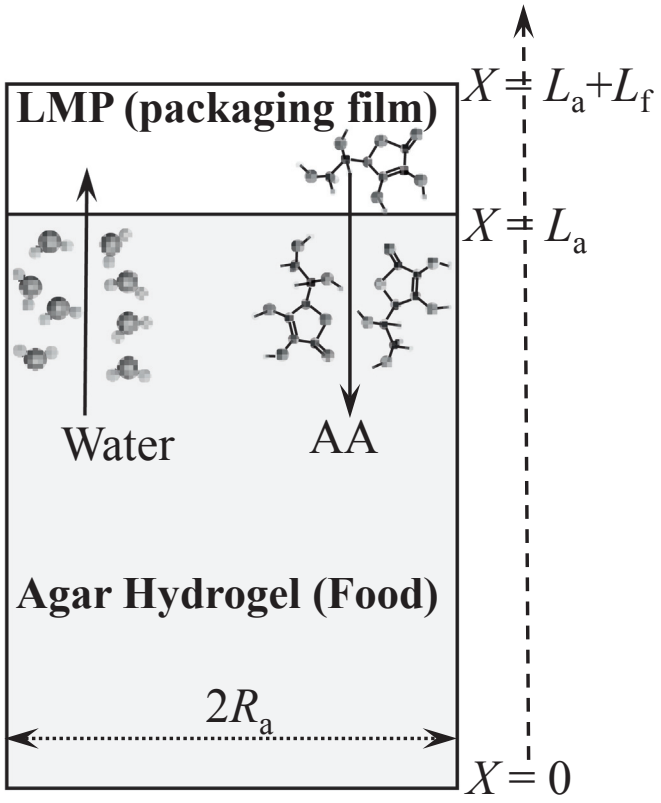

Fig. 1. A LMP film (packaging), L_f thick, lies on the top of an agar hydrogel cylinder (food) of radius R_a and thickness L_a. Water molecules, leaving the hydrogel due to a chemical potential difference, swell the initially dry LMP film. The film swelling, in turn, promotes the ascorbic acid (AA) dissolution and transport through the LMP film toward the agar hydrogel. X represents the axial coordinate.

2.1. LMP film

2.1.1. Water

In the light of the aforementioned hypotheses, although other approaches could have been considered (for example, the dependence of the water diffusion coefficient on system viscosity), the transport equation for water may be represented as follows (Cohen and White, 1991; Edwards and Cohen, 1995):

$$\frac{\partial C_{wf}}{\partial t} = -\frac{\partial}{\partial X}(J_F + J_{NF}) = \frac{\partial}{\partial X}\left(D_{wf}\frac{\partial C_{wf}}{\partial X} + D_v\frac{\partial \sigma}{\partial X}\right) \quad (1)$$

where t is time, X is the axial coordinate, C_{wf} is the water local concentration (mass/volume), J_F and J_{NF} are the Fickian and non-Fickian water flows, respectively, D_{wf} and D_v (dimensionally, a time) are the water diffusion and viscoelastic diffusion coefficients, respectively, while σ is the stress generated by the incoming water in the film network. Fundamentally, eq. (1) derives from the assumption that the water chemical potential depends on both concentration (C_{wf}) and stress (σ). Although, in principle, σ is a tensor, it may be regarded as a scalar representing an osmotically-induced viscoelastic swelling pressure related to the trace of the stress tensor in the LMP network (Swaminathan and Edwards, 2004). Indeed, one-third of the tensor trace represents the normal stress appearing in the tensor spherical (or hydrostatic) part. Thus, the non-Fickian component (J_{NF}) of water flow is due to σ. According to Ferreira et al. (2014), σ may be properly described by a generalized Maxwell's model, a series combination of an elastic element and N viscoelastic ones:

$$\sigma = \sigma_0 + \sum_{i=1}^{N} \sigma_i \quad (2)$$

$$\sigma_0 = -E_0\varepsilon \quad (3)$$

$$\frac{d\sigma_i}{dt}+\frac{\sigma_i}{\lambda_i}=-\frac{d\varepsilon}{dt}E_i \quad i=1\rightarrow N \tag{4}$$

$$E_i=E_{mi}\frac{\rho-C_{wf}}{\rho-C_m} \qquad i=0\rightarrow N \tag{5}$$

$$\lambda_i=\lambda_{ei}e^{\left(k\left(1-C_{wf}/C_{ef}\right)\right)} \quad i=1\rightarrow N \tag{6}$$

$$\varepsilon=\left(\frac{\rho-C_R}{\rho-C_{wf}}\right)\frac{C_{wf}}{\rho}-\frac{C_R}{\rho} \tag{7}$$

where σ_0 and E_0 are, respectively, the stress and the elastic modulus of the elastic element, ε is the local deformation (a simple approximation of the deformation tensor), ρ is the solvent density, σ_i, E_i, and λ_i represent, respectively, the stress, the elastic modulus, and the relaxation time of the generic viscoelastic element, k is a model parameter, C_{ef} indicates the solvent concentration in the fully swollen film (thermodynamic equilibrium), while λ_{ei} is the value assumed by λ_i at equilibrium (i.e. when $C_{wf}=C_{ef}$). The "minus" sign appearing in eqs. (3) and (4) remembers that stress (σ) is opposite to deformation (ε). The linear dependence of E_i on C_{wf} (eq. (5)) is a direct consequence of Flory's theory (Flory, 1953). Indeed, according to Flory, the crosslink density (ρ_x), defined as the moles of junctions among the different chains constituting the polymeric network per unit volume, varies with C_{wf} linearly. In addition, by resorting to the same theory, the elastic modulus (Young's modulus) is proportional to ρ_x through 3RT (R = universal gas constant, T = absolute temperature). Thus, in the present work, it is assumed that the E_i dependence on C_{wf} ($i=0$ to N) may be described by eq. (5), where C_m is the uniform water concentration in the film corresponding to the condition of the (rheological) determination of each E_{mi}. Finally, eq. (7) implies that no deformation (and, hence, stress) occurs when C_{wf} equals the solvent concentration (C_R) corresponding to the crosslinking conditions (if $C_R=0$, the expression employed by Ferreira et al. (2015) may be derived).

A Fujita-type exponential dependence for the solvent diffusion coefficient, D_{wf}, was considered (Grassi et al., 2007):

$$D_{wf}=D^e_{wf}\exp\left(-\beta_{wf}\left(1-\frac{C_{wf}}{C_{ef}}\right)\right) \tag{8}$$

where D^e_{wf} is the equilibrium value of D_{wf} (i.e. when $C_{wf}=C_{ef}$) and β_{wf} is a model parameter to be determined.

Although other possibilities exist (Ferreira et al., 2015), the evaluation of the viscoelastic diffusion coefficient, D_v, was performed according to Darcy's theory (Truskey et al., 2004), which assimilates a polymeric network to a porous system:

$$D_v=C_{wf}\alpha^3 r_f^2\Big/\left(4g\eta\left(1-\alpha^2\right)\right)\quad \alpha=C_{wf}/\rho \tag{9}$$

$$g=\frac{2}{3}\frac{\alpha^3}{(1-\alpha)}\left[\frac{1}{-2\ln(1-\alpha)-3+4(1-\alpha)-(1-\alpha)^2}+\frac{2}{-\ln(1-\alpha)-\frac{1-(1-\alpha)^2}{1+(1-\alpha)^2}}\right] \tag{10}$$

where α is the system porosity, η is the water viscosity at a fixed temperature, and r_f is the radius of the chains (assumed of cylindrical shape) constituting the polymeric network. Fundamentally, Darcy's theory provides a sigmoidal increase (in a bi-logarithmic diagram) of D_v with C_{wf}.

In order to consider the LMP film swelling, an isotropic volume increase was introduced (Grassi et al., 2007):

$$\frac{R_f}{R_{f0}}=\frac{dX}{dX_0}=1\Big/\sqrt[3]{1-C_{wf}/\rho} \tag{11}$$

where R_f and dX indicate, respectively, the radius and the thickness of the generic film slice, while R_{f0} and dX_0 correspond to R_f and dX in the initial dry condition.

2.1.2. Ascorbic acid

The transport equation relative to AA reads:

$$\frac{\partial C_{df}}{\partial t}=K_t\left(1-\frac{C_{df}}{C_s}\right)C_{wf}-K_{df}C_{df}+\frac{\partial}{\partial X}\left(D_{df}\frac{\partial C_{df}}{\partial X}-vC_{df}\right) \tag{12}$$

where C_{df} and C_s denote, respectively, the AA local concentration (mass/volume) and the AA saturation concentration in the LMP film, D_{df} is the AA diffusion coefficient in the LMP film, K_t and K_{df} represent, respectively, the AA dissolution and degradation constants, while v is velocity.

Eq. (12) describes the most important phenomena affecting the AA fate once the LMP film is placed in contact with the agar hydrogel. Indeed, as AA is initially present in the dry LMP film in a solid state, its movement through the polymeric network may occur on condition that it dissolves in the incoming water. The first right-hand side term of eq. (12) portrays this phenomenon and sets the AA dissolution kinetics to zero when the water local concentration (C_{wf}) is zero or the AA local concentration (C_{df}) equals the saturation threshold (C_s) (Grassi et al., 2007; Ferreira et al., 2015). The reduction of the solid AA local concentration (C_t) is, then, given by:

$$\frac{\partial C_t}{\partial t}=-K_t\left(1-\frac{C_{df}}{C_s}\right)C_{wf} \tag{13}$$

Obviously, eq. (13) and the first right-hand side term of eq. (12) disappear if the C_t local value becomes zero. Being a well-known fact that AA undergoes degradation in water (León and Rojas, 2007), the second right-hand side term of eq. (12) assumes an AA linear degradation kinetics.

The last right-hand side term of eq. (12) represents the AA transport due to the existence of a concentration gradient and a convective field (v) induced by the stress gradient caused by the water uptake from the agar hydrogel. Indeed, by assuming that the stress gradient acts similarly to a pressure gradient inside a pipe, the non-Fickian water flow may be regarded as the cause of a convective field defined by:

$$J_{NF}=-D_v\frac{\partial\sigma}{\partial X}=vC_{wf} \tag{14}$$

The D_{df} dependence on C_{wf} is assumed exponential as suggested by the major theories aimed at estimating the solute diffusivity in polymeric matrices (Grassi et al., 2007):

$$D_{df}=D^0_{df}\exp\left(\beta_{df}\left(1-\frac{\rho}{C_{wf}}\right)\right) \tag{15}$$

where D^0_{df} is the AA diffusion coefficient in pure water, while β_{df} is a model parameter to be determined.

2.2. Agar hydrogel

2.2.1. Water

Although, in principle, eqs. (1) and (12) may be applied to describe the water and AA transport, some important simplifications shall be considered as, in the experimental setup which the present investigation refers to, the volume of agar hydrogel is always much larger than the LMP film one (>36 times). Thus, during the whole experiment, the reduction of the agar hydrogel mass and volume due to the water transport to the LMP film is negligible. Consequently, the agar hydrogel deformation is always very small and this translates into a negligible stress field. Therefore, eq. (1) may be simplified into a classic Fickian diffusive transport:

$$\frac{\partial C_{wa}}{\partial t} = \frac{\partial}{\partial X}\left(D_{wa}\frac{\partial C_{wa}}{\partial X}\right) \tag{16}$$

where C_{wa} and D_{wa} represent, respectively, the water concentration and the diffusion coefficient inside the agar hydrogel. Again, D_{wa} may be evaluated according to a Fujita-type exponential dependence on C_{wa}:

$$D_{wa} = D^{e}_{wa}\exp\left(-\beta_{wa}\left(1-\frac{C_{wa}}{C_{ea}}\right)\right) \tag{17}$$

where C_{ea} is the water concentration in the agar hydrogel at the thermodynamic equilibrium, D^{e}_{wa} is the equilibrium value of D_{wa} (i.e. when $C_{wa} = C_{ea}$), and β_{wa} is a model parameter to be determined.

2.2.2. Ascorbic acid

With regard to the AA transport also, eq. (12) may be simplified as the convective field is vanishingly small and the AA dissolution is prevented since no solid AA may be present in the agar hydrogel. Thus, eq. (12) becomes:

$$\frac{\partial C_{da}}{\partial t} = -K_{da}C_{da} + \frac{\partial}{\partial X}\left(D_{da}\frac{\partial C_{da}}{\partial X}\right) \tag{18}$$

where C_{da} denotes the AA local concentration (mass/volume), D_{da} and K_{da} are, respectively, the AA diffusion coefficient and degradation constant in the agar hydrogel.

The D_{da} dependence on C_{wf} is, again, assumed exponential (Grassi et al., 2007):

$$D_{da} = D^{0}_{da}\exp\left(\beta_{da}\left(1-\frac{\rho}{C_{wa}}\right)\right) \tag{19}$$

where D^{0}_{da} is the AA diffusion coefficient in pure water, while β_{da} is a model parameter to be determined.

2.3. Initial and boundary conditions

2.3.1. Initial conditions

Eqs. (1), (12), (16) and (18) are solved by assuming that, at the beginning, the water concentration is zero throughout the LMP film ($C_{wf0} = 0$), while it is equal to the thermodynamic equilibrium value throughout the agar hydrogel ($C_{wa0} = C_{ea}$). On the contrary, the initial concentration of AA is set to zero in the agar hydrogel ($C_{da0} = 0$) and to a finite value in the LMP film (C_{df0}).

2.3.2. Boundary conditions

With regard to water (eqs. (1) and (12)), the impermeable wall condition is set for $X = 0$ ($\nabla C_{wa} = 0$) and $X = L_a + L_f$ ($\nabla C_{wf} = 0$) (see Fig. 1). On the contrary, a thermodynamic equilibrium condition is assumed for the water concentration at the agar hydrogel/LMP film interface:

$$\left.\frac{C_{wa}}{C_{wf}}\right|_{X=L_a} = k_{pw} \tag{20}$$

where k_{pw} is the partition coefficient. Furthermore, an overall water mass balance is considered to evaluate C_{wa} ($X = L_a$):

$$M_{w0} = S_a\int_0^{L_a} C_{wa}dX + \int_{L_a}^{L_a+L_f} S_f C_{wf}dX \tag{21}$$

where M_{w0} is the water amount initially present in the agar hydrogel, S_a and S_f are, respectively, the agar hydrogel and film cross sections, while L_a and L_f are, respectively, the agar hydrogel and film thicknesses (see Fig. 1). Eq. (21) ensures that the water amount inside the system composed of the LMP film in contact with the agar hydrogel is constant during the entire transport experiment.

Finally, the boundary conditions regarding the AA transport (eqs. (16) and (18)) imply the impermeable wall ones for $X = 0$ ($\nabla C_{da} = 0$) and $X = L_a + L_f$ ($\nabla C_{df} = 0$) (see Fig. 1). Moreover, the AA concentration at the agar hydrogel/LMP film interface is evaluated by assuming the same partitioning condition expressed by eq. (20) and an overall mass balance similar to that expressed by eq. (21):

$$\left.\frac{C_{da}}{C_{df}}\right|_{X=L_a} = k_{pd} \tag{22}$$

$$M_{d0} = S_a\int_0^{L_a} C_{da}dX + \int_{L_a}^{L_a+L_f} S_f\left(C_{df}+C_t\right)dX + \int_0^{t}\int_0^{L_a+L_f} K_{da}C_d\,dt\,dX \tag{23}$$

where k_{pd} is the AA partition coefficient and M_{d0} is the initial AA amount present in the dry LMP film. The double integral describes the degraded AA amount in the film/hydrogel system up to the time t, being C_d equal to C_{da} or C_{df} depending on position.

2.3.3. Numerical solution

The model equations (eqs. (1), (12), (16) and (18)) were numerically solved by means of an ad hoc FORTRAN program implementing the implicit control volume method (Patankar, 1990). The resulting nonlinear system of equations was iteratively solved (relative tolerance = 10^{-6}) through Gauss-Seidel's method (Chapra and Canale, 1998). The LMP film thickness was subdivided into 10 control volumes, while the agar hydrogel one into 40 control volumes. The discretization time step was set to 10^{-2} s.

3. Materials and methods

3.1. Chemicals

L-(+)-ascorbic acid and potassium sorbate were supplied by Sigma-Aldrich (Saint Louis, USA). LMP was supplied by CP Kelco (GENUTM pectin type LM-12 CG, USA). Agar was supplied by Biokar (Diagnostics, France). Glycerol and $CaCl_2{}^{\circ}2H_2O$ were supplied by Merck (Argentina).

3.2. Agar cylinders

The agar cylinders were produced by dissolving 2 g of agar in

sufficient distilled water (approximately 90 mL) at a temperature of 90 °C. Then, the total weight was increased to 100 g in a scale (0.01 g precision). After homogenization, the solution was poured into a cylindrical container (L_a = height = 2 cm, $2R_a$ = diameter = 2.2 cm; see Fig. 1) and allowed to cool in order to gel.

3.3. LMP film formation

The LMP films were prepared according to the casting technology. For this purpose, an amount of 8.00 g of LMP powder was slowly poured in 250 g of deionized water under high stirring conditions (1400 rpm) ensured by a vertical stirrer (model LH, Velp Scientifica, Italy) to prevent the formation of lumps and obtain a homogeneous powder hydration. The obtained viscous, homogenous, and transparent system was, then, heated to 90 °C on a hotplate at a constant heating rate (5 °C/min). Glycerol was added (5.00 g) as a plasticizer, followed by potassium sorbate (0.0300% w/w) as an antimicrobial and AA (0.1% w/w), both predissolved in approximately 10 mL of deionized water. When temperature returned to 90 °C, $CaCl_2{}^{\circ}2H_2O$, predissolved in approximately 10 mL of deionized water, was added while stirring. The total weight of the system was, then, increased to 300 g by adding sufficient deionized water while stirring for homogenization. The foam formed in the hot solution was removed with a spatula. The hot solution underwent vacuum treatment for 15 s to eliminate bubbles and, then, was poured onto leveled polystyrene plates (7 g of solution per 55 mm-diameter polystyrene plate). The plates were cooled for 20 min at room temperature in order to gel the supported solution and, then, air-dried in a convection oven for 2.5 h at 60 °C. The obtained films were cooled at room temperature, peeled from the polystyrene plates, and stored under vacuum in Cryovac™ bags (Sealed Air, USA). The final dry film thickness (L_f) was approximately 100 μm and the AA concentration (C_{df0}) was 30.4 kg/m^3.

3.4. Mass transport test

Each experiment consisted in placing six films (100 μm thick and 2.2 cm in diameter) on six agar hydrogel cylinders (2 cm high, 2.2 cm in diameter, agar 2% w/w). At time zero, these systems (cylinder + LMP film) were placed in a sealed container maintained at a constant temperature (25.0 °C) and an almost constant humidity by employing a water-soaked gauze. At each time point (0.25, 0.75, 1.5, 4, 6, and 8 h), one system was withdrawn in order to separately weigh the LMP film and the corresponding hydrogel cylinder thus following the kinetics of water gain/loss. Then, the film and the hydrogel cylinder, cut into four pieces (0.5 cm thick), were sacrificed to determine the AA content. The LMP film and the four hydrogel parts were initially cut into smaller parts (less than 1 mm) and, then, separately placed in 20 mL volumetric flasks containing a 1% (w/v) oxalic acid solution under vortexing (35 Hz, Velp, Italy) for 120 s to achieve the total extraction of AA. The resulting suspension was finally stored at 4 °C for 30 min. An aliquot was withdrawn from the supernatant and the AA concentration was determined by using the 2,6 dichlorophenolindophenol spectrophotometric method (De'Nobili et al., 2013). The AA concentration was determined in two different aliquots (duplicate) for every film and piece of the cylindrical samples. The experiment was performed in triplicate.

3.5. Ascorbic acid degradation kinetics

As the AA degradation is induced by the presence of water, the AA loaded LMP films were stored in a desiccator characterized by a constant relative humidity (*RH*%) of 100% at 25 °C (Favetto et al., 1983; Greenspan, 1977) assured by the presence of a saturated aqueous solution of K_2SO_4 (water activity (Wa°) of 0.974). The equilibration was assessed by measuring the film water activity (Wa) up to the attainment of Wa°, corresponding to $RH\% = 100$. At fixed intervals, the films were withdrawn from the desiccator in order to determine the AA concentration. Accordingly, the sampled film was firstly cut into smaller pieces than 1 mm in size, weighed in an analytical scale (0.0001 g), placed in a 25 mL volumetric flask containing a 1% (w/v) oxalic acid solution, and magnetically stirred for 1.5 h at 5 °C to achieve the total extraction of AA from the film. In order to improve the extraction, every 15 min, stirring was interrupted and the suspension underwent vortexing for 90 s at 35 Hz (Velp, Italy). The suspension was finally centrifuged at 10.000 rpm and 6 °C for 30 min (Eppendorf 5810R Refrigerated Centrifuge, USA). A supernatant aliquot was sampled and the AA concentration was determined by employing the 2,6-dichlorophenolindophenol spectrophotometric method (De'Nobili et al., 2013). The AA concentration was determined in two different aliquots (duplicate) for every film sample. The experiment was performed in triplicate.

4. Results and discussion

As the objective of the proposed model was to perform a reliable prediction of the AA transport from packaging (LMP film) to food (agar hydrogel), the preliminary determination of all the model parameters was necessary. Table 1 displays the list of the model parameters and the way they were determined, i.e. measured, assumed, set, known, and evaluated.

Thus, the first aspect to consider was the determination of the viscoelastic properties of the LMP film, which, upon contact with the swollen agar hydrogel, starts absorbing water (swelling). The rheological characterization performed by De'Nobili et al. (2015) revealed that five Maxwell's elements were necessary to describe the mechanical spectra of the swelling LMP film: a purely elastic element (G_0) and four viscoelastic ones (G_1-λ_1, G_2-λ_2, G_3-λ_3, G_4-λ_4, see Table 1). As the rheological characterization was conducted under shear conditions and the present model is referred to normal stresses (see eqs. (2)–(5)), the conversion from shear to normal stress moduli was performed by resorting to the linear viscoelasticity principles (Lapasin and Pricl, 1995). Indeed, by assuming that the swelling LMP film is incompressible, the linear viscoelastic theory ensures that $E_i = 3G_i$ ($i = 0 - N$). By adopting a consolidated approach (Lapasin and Pricl, 1995), the couples (G_i-λ_i) were determined by assuming that each λ_i was scaled by a factor of ten, while the most probable number of Maxwell's elements was determined according to a statistical procedure described in De'Nobili et al. (2015). Interestingly, despite the fact that both E_i (= $3G_i$) and λ_i should be dependent on the solvent (water) concentration (see eqs. (5) and (6), respectively), De'Nobili et al. (2015) discovered that, regardless of the solvent concentration in the LMP film, the E_0 and (E_i-λ_i) values scattered around the mean values displayed in Table 1 without showing any particular trend. Accordingly, in the present work, their values were assumed constant during the LMP film swelling process (this meant setting $C_m = C = C_{wf}$ in eq. (5) and $k = 0$ in eq. (6)), even if, at least at the beginning of the process, the E_i reduction with water concentration occurs. The low field nuclear magnetic resonance (LF-NMR) characterization performed by De'Nobili et al. (2015) confirmed the almost constant properties of the swelling LMP film as the values of the water diffusion coefficient (D_{wf}) in the film is almost independent of the solvent concentration (i.e. the swelling time) at least for $t \geq 0.25$ h. As a consequence, in eq. (8), D^e_{wf} was set to $1.5{*}10^{-9}$ m^2/s, as shown in Table 1. In order to consider the initial stage of the LMP film swelling process also, when the rheological and LF-NMR characterizations were practically unattainable, the LMP film weight

Table 1
Values of the model parameters.

LMP-FILM			
Water			
E_i (Pa) = 3 G_i(Pa)	$E_0 = 3\ G_0 = 32972$ $E_1 = 3\ G_1 = 85438$ $E_2 = 3\ G_2 = 54674$ $E_3 = 3\ G_3 = 43378$ $E_4 = 3\ G_4 = 76791$	Eq. (5)	measured
λ_i (s)	λ_1 (s) = 4.7*10^{-2} λ_2 (s) = 4.7*10^{-1} λ_3 (s) = 4.7*10^{0} λ_4 (s) = 4.7*10^{1}	Eq. (6)	measured
k (−)	0	Eq. (6)	assumed
C_{ef} (kg/m^3)	987	Eq. (6)	assumed
C_{ea} (kg/m^3)	987	Eq. (17)	assumed
C_m (kg/m^3)	987	Eq. (5)	assumed
C_R (kg/m^3)	987	Eq. (7)	set
ρ (kg/m^3)	1000	–	known
D^e_{wf} (m^2/s)	1.5*10^{-9}	Eq. (8)	measured
β_{wf} (-)	15	Eq. (8)	evaluated
r_f (m)	10^{-9}	Eq. (9)	Amsden 1998
η_s (Pa s) 25 °C	≈10^{-3}	Eq. (9)	Lapasin and Pricl 1995
L_f (m)	10^{-4}	Fig. 1	set
C_{wf0} (kg/m^3)	0	–	set
k_{pw} (-)	1	Eq. (20)	assumed
AA			
K_t (s^{-1})	5.4*10^{-3}	Eq. (12)	evaluated
C_s (kg/m^3)	330	Eq. (12)	Shalmashi and Eliassi 2008
K_{df} (s^{-1})	4.3*10^{-6}	Eq. (12)	measured
D_{df} (m^2/s)	1.5*10^{-9}	Eq. (15)	assumed
C_{df0} (kg/m^3)	30.4	–	set
k_{pd} (-)	1	Eq. (22)	assumed
M_{d0} (μg)	1300	Eq. (23)	set
AGAR HYDROGEL			
Water			
β_{wa} (-)	15	Eq. (16)	evaluated
D^e_{wa} (m^2/s)	1.8*10^{-9}	Eq. (17)	measured
C_{ef} (kg/m^3)	987	Eq. (17)	assumed
M_{w0} (kg)	7.5*10^{-3}	Eq. (21)	set
L_a (m)	2*10^{-2}	Fig. 1	set
R_a (m)	1.1*10^{-2}	Fig. 1	set
AA			
K_{da} (s^{-1})	2.5*10^{-6}	Eq. (18)	measured
D_{da} (m^2/s)	1.4*10^{-9}	Eq. (19)	measured
C_{da0} (kg/m^3)	0		set

increase and the agar hydrogel weight decrease were recorded over 8 h (Fig. 2). Then, eqs. (1) and (16) were fitted to these experimental data thus assuming β_{wf} and β_{wa} as the unique fitting parameters (all other parameters values in eqs. (1) and (16) were those displayed in Table 1, thus assuming $C_{ef} = C_{ea} = 987$ kg/m^3 as the swollen film and the swollen agar are thermodynamically and structurally not so dissimilar and 987 represents, approximately, the water concentration in the just formed agar gel (= food)). The fitting procedure led to $\beta_{wf} = \beta_{wa} = 15$ and a satisfactory data description, as witnessed by Fig. 2.

In order to evaluate the water viscoelastic diffusion coefficient inside the LMP film (D_v), Darcy's approach, represented by eqs. (9) and (10), required the knowledge of water viscosity (η) and polymeric chain radius r_s (in this theory, polymeric chains are assumed as very long cylinders with radius r_s). While η at 25 °C is well-known, the r_s value was chosen among those typical for these polymeric systems (Amsden, 1998). The last model parameter relative to the LMP film/water component, the partition coefficient (k_{pw}), was set to 1 as, thermodynamically speaking, the LMP film and the agar hydrogel are similar. Thus, it seemed unreasonable to have different water concentrations at the two sides of the LMP film/agar hydrogel interface.

Although the determination of the AA dissolution constant (K_t) inside a polymeric network is a challenging task, its order of

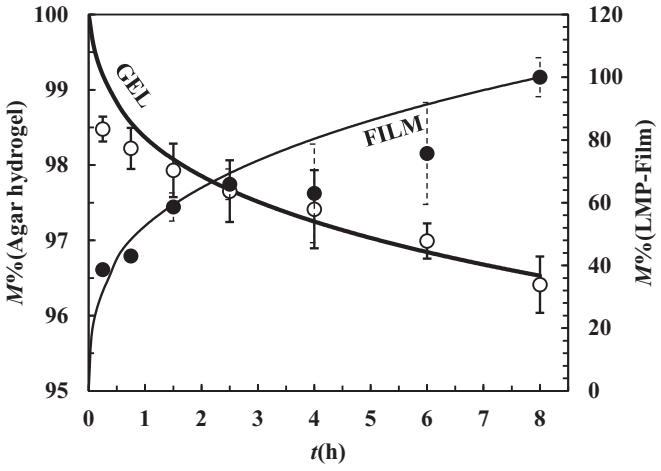

Fig. 2. Relative weight decrease/increase of the agar hydrogel/LMP film (*M*%). The black and white circles refer, respectively, to the agar hydrogel weight decrease and the LMP film weight increase. The solid lines indicate the model best fitting (eqs. (1) and (16)) to the experimental data, whose standard deviations are represented by vertical bars. *t* is time (hours). The data variation coefficient *CV* concerning the agar hydrogel weight decrease ranges from 0.2 to 0.5, while *CV* concerning the LMP film weight increase ranges from 3.8 to 25.0.

magnitude may be estimated according to Levich's theory (Levich, 1962). This theory states that the mass transfer coefficient (the intrinsic dissolution constant, k_{diss}) between a solid phase and a liquid one in relative motion is described by:

$$k_{diss} = 0.6271 D^{2/3} \eta^{1/6} \omega^{1/2} \quad (24)$$

where D is the diffusion coefficient of the solid molecules in the liquid phase, η is the liquid viscosity, and ω is the relative angular velocity between the liquid and solid phases. In the light of the relation existing between k_{diss} and K_t (Grassi et al., 2007):

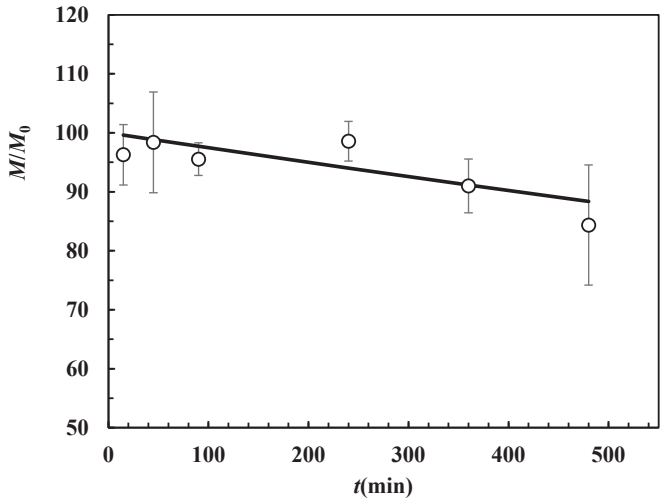

Fig. 3. Model best fitting (solid line, eq. (26)) to the experimental data (symbols) referring to the ascorbic acid (AA) degradation (M/M_0) in the LMP film at 25 °C and 100% relative humidity. The vertical bars indicate the data standard deviations. The data variation coefficient (*CV*) ranges from 2.9 to 12.1.

$$K_t = \frac{3 C_{df0}}{R_p \rho_{solid}} k_{diss} \quad (25)$$

where R_p is the radius of the solid particles and ρ_{solid} is the solid density, it was possible to estimate K_t. By knowing that $\eta = 10^{-3}$ Pa s, $D = 1.5{*}10^{-9}$ m^2/s $= D_{df}$ (the AA diffusion coefficient in the film, see Table 1), $R_p \approx 10$ μm, $\rho_{solid} = 1650$ kg/m^3, $C_{df0} = 30.4$ kg/m^3 (see Table 1), and by assuming that $\omega \approx 0.1$ rad/s (a very low value that should approximate the relative velocity between the solid and liquid phases embedded in the polymeric network), $K_t \approx 5{*}10^{-4}$ s^{-1} was obtained. The second important parameter regarding AA is its degradation constant inside the LMP film (K_{df}) and the agar hydrogel (K_{da}). As the two environments (LMP film and agar hydrogel) are similar, it was assumed that $K_{df} = K_{da}$. The determination of the AA dissolution constant was performed by fitting degradation data (see Fig. 3) by means of the linear model assumed in eq. (12), whose macroscopic expression reads:

$$M/M_0 = e^{-K_{df} t} \quad (26)$$

where M is the un-degraded AA amount at time t, while M_0 is its initial value. Eq. (26) fitting led to $K_{df} = K_{da} = 4.3{*}10^{-6}$ s^{-1}.

As the determination of the AA diffusion coefficient (D_{df}) in the swelling film is a challenging task, a simplified approach was adopted. Thus, it was assumed that $D_{df} \approx D_{da}$ (the AA diffusion coefficient in the agar hydrogel), being both independent of water concentration. Hence, D_{da} evaluation was performed by following the procedure described in section 3.4 *Mass transport test* by simply substituting the LMP film for an AA aqueous solution (initial concentration (C_{sol0}) of 14 kg/m^3, volume (V_{sol}) of 100 μl) containing, approximately, the same AA amount present in the dry LMP film ($M_{d0} = 1300$ μg). By assuming that the aqueous solution was a well-stirred environment (this is reasonable in the light of its small

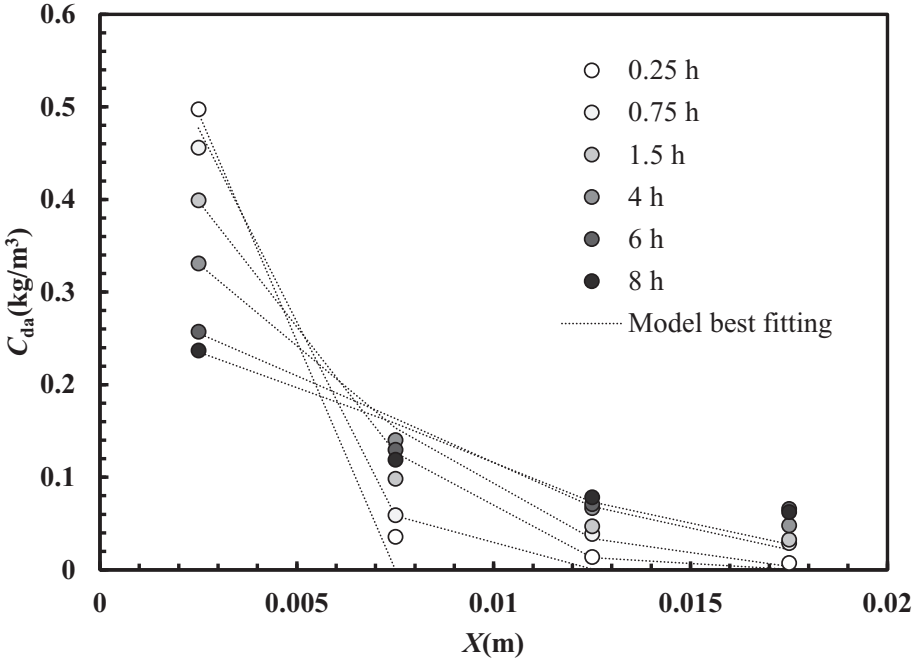

Fig. 4. Determination of the ascorbic acid (AA) diffusion coefficient inside the agar hydrogel. The dotted lines represent the model best fitting (eq. (18)) to the experimental data (symbols), i.e. the AA concentration (C_{da}) profile in the agar hydrogel at different times. In this experiment, the AA loaded LMP film placed on the top of the agar hydrogel was replaced by an aqueous solution containing the same AA amount. *X* indicates the axial coordinate. The average data variation coefficient (*CV*) is equal to 75, 29, 24, 24, 13 and 24 for the concentration profiles data at 0.25, 0.75, 1.5, 4, 6, and 8 h, respectively.

thickness (L_{sol}) of 250 μm), the diffusion process was modelled according to eq. (18) by assuming $k_{pd} = 1$ (as both the agar and the film are, from a thermodynamic viewpoint, similar, the AA concentration on both the interface sides should be the same), the impermeable wall condition for $X = 0$ (see Fig. 1), and the following global mass balance:

$$V_{sol}C_{sol0} = S_a\int_0^{L_a} C_{da}dX + V_{sol}C_{sol}(t) + S_a\int_0^t\int_0^{L_a} K_{da}C_{da}dtdX + \int_0^t K_{da}C_{sol}(t)dt \quad (27)$$

Eq. (27) states that the initial AA amount in the solution ($V_{sol}C_{sol0}$) must be always equal to the sum of a) the AA amount still present in the agar hydrogel (first right-hand side term), b) the AA amount still present in the solution (second right-hand side term), c) the AA amount degraded in the agar hydrogel (third right-hand side term), and d) the AA amount degraded in the solution (fourth right-hand side term). Fig. 4 shows the comparison between the model best fitting (lines) and the experimental concentration profiles (symbols) after 0.25 h, 0.75 h, 1.5 h, 4 h, 6 h, and 8 h. This fitting led to different D_{da} values at different times: $0.8*10^{-9}$ m^2/s (0.25 h), $1.9*10^{-9}$ m^2/s (0.75 h), $1.9*10^{-9}$ m^2/s (1.5 h), $1.1*10^{-9}$ m^2/s (4 h), $1.3*10^{-9}$ m^2/s (6 h), and $1.1*10^{-9}$ m^2/s (8 h). Consequently, it was decided to consider the average value displayed in Table 1. Finally, the water diffusion coefficient in the agar hydrogel was evaluated through LF-NMR (De'Nobili et al., 2015). Its equilibrium value (D^e_{wa}) was equal to $1.8*10^{-9}$ m^2/s (see Table 1).

By relying on the parameters displayed in Table 1, the proposed model was employed to predict the time evolution of the AA amount in the system formed by the packaging (LMP film) in contact with food (agar hydrogel). Fig. 5A shows the comparison between the model prediction (dotted lines) and the experimental data (symbols) referring to the time evolution of the AA amount (M_A) present in the LMP film and in the four zones which agar hydrogel was subdivided into. Although the data standard deviations were hidden for the sake of clarity, it is clear that the model prediction is more than satisfactory as it is close to the experimental trend whatever the considered time point is. This statement is supported by Fig. 5B depicting the time evolution of the total AA amount inside the agar hydrogel (M_{AG}). It appears that the model prediction (solid line) differs from the experimental data (symbols) less than one standard deviation except for the first zone (the one in contact with the LMP film). The comparison between the model prediction and the experimental data is even better in the case of the AA amount (M_{AF}) time evolution inside the LMP film. Indeed, Fig. 5C demonstrates that the model prediction (solid line) detaches from the experimental data (symbols) less than a standard deviation in the whole course of the considered time.

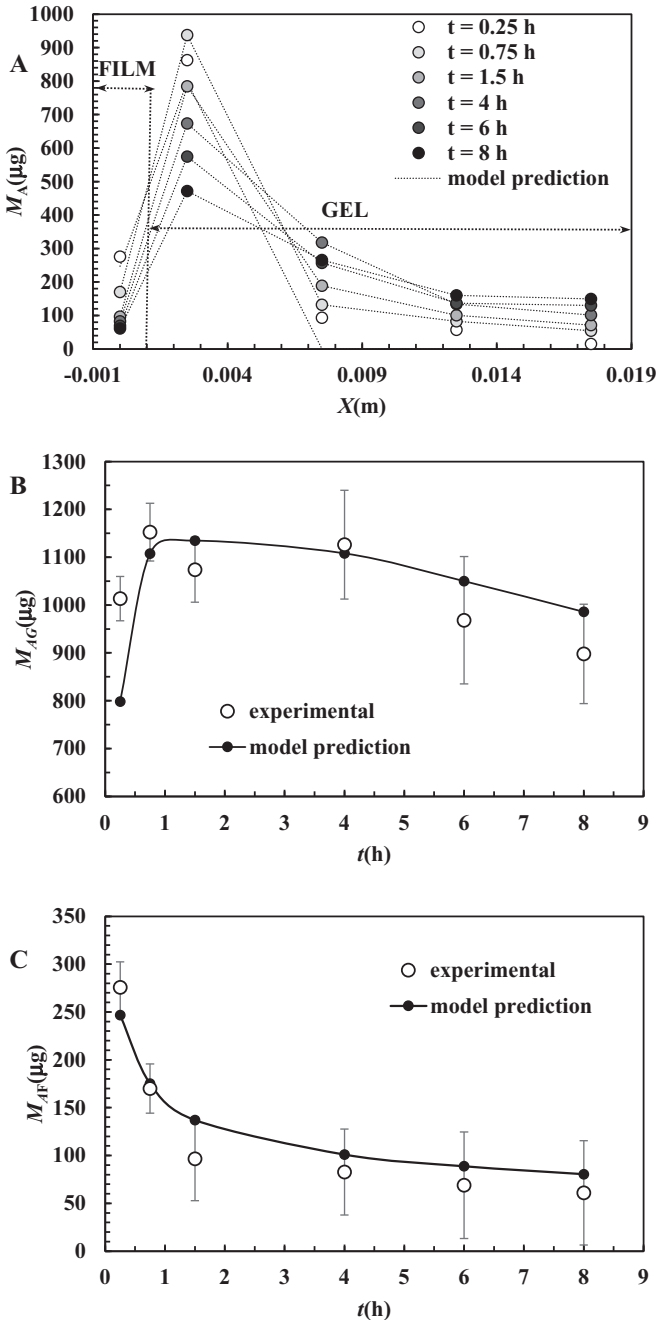

Fig. 5. A) Comparison between the model prediction (dotted lines) and the experimental data (symbols) referring to the variation of the ascorbic acid (AA) concentration (C_{da}) inside the LMP film and the agar hydrogel at different times. The average data variation coefficient (*CV*) is equal to 7, 25, 20, 25, 30 and 32 for the concentration profiles at 0.25, 0.75, 1.5, 4, 6, and 8 h, respectively. **B)** Comparison between the model prediction (solid line and black dots) and the experimental data (white circles) referring to the variation of the ascorbic acid (AA) amount (M_{AG}) in the agar hydrogel at different times. *CV* ranges from 9 to 89. **C)** Comparison between the model prediction (solid line and black dots) and the experimental data (white circles) referring to the variation of the ascorbic acid (AA) amount (M_{AF}) in the LMP film at different times. *CV* ranges from 4.6 to 11.6. The vertical bars indicate the data standard deviations, while *t* is time (hours).

5. Conclusions

The proposed model, aimed at describing the AA transport from an LMP film (packaging) to an agar hydrogel (food), proved to be reliable as it was able to satisfactorily predict experimental data. This, indirectly, witnessed that all the considered simplifying hypotheses were, substantially, reasonable and physically sound. Obviously, while the model strength resides in the possibility of measuring/estimating all its parameters, the determination of so many parameters may be considered a small drawback. Nevertheless, as the determined parameters may be assumed as average values for typical packaging (polymeric) films and food, the values displayed in Table 1 may be roughly employed to predict the AA penetration into a great variety of different situations provided that the geometrical details and the initial conditions of the packaging-food system are known. In addition, the model running is

timesaving as approximately 3 min were necessary for simulating an eight hours laboratory session on an *Intel® Core™ i7-3540M* CPU @ 3 GHz, 4 GB RAM, computer.

Finally, it could be verified that, in the light of the adopted AA degradation constant, the effect of degradation is reflected in a significant variation of the AA amount in the agar hydrogel (up to 12%) only after 0.5 h. On the contrary, the effect of viscoelasticity and drug dissolution becomes important (up to 156% and 800%, respectively) within the first 0.5 h. This means that, for longer times, it may be safely assumed that the solvent transport is chiefly ruled by diffusion inside the film also. Similarly, the assumption of an instantaneous AA dissolution ($K_t \rightarrow \infty$) inside the film is acceptable if the simulation target exceeds, approximately, 0.5 h.

In conclusion, the presented model proved to be a reliable tool for designing packaging polymeric films aimed at releasing antioxidant agents like AA.

Acknowledgments

Gianluca Chiarappa, Michela Abrami, Romano Lapasin, Gabriele Grassi, and Mario Grassi wish to thank the Italian Ministry of Education (PRIN 2010-11 (20109PLMH2)). Maria De'Nobili and Ana Rojas are grateful to the University of Buenos Aires, National Research Council of Argentina (CONICET), and Agencia Nacional de Promoción Científica y Tecnológica (ANPCyT). J. A. Ferreira and Paula de Oliveira thank the partial support of the Center for Mathematics of the University of Coimbra-UID/MAT/00324/2013, funded by the Portuguese Government through FCT/MEC and co-funded by the European Regional Development Fund through the Partnership Agreement PT2020.

References

Amsden, B., 1998. Solute diffusion within hydrogels. Mechanisms and models. Macromolecules 31, 8382–8395.
Baldwin, E.A., Nisperos, M.O., Chen, X., Hagenmaier, R.D., 1996. Improving storage life of cut apple and potato with edible coating. Postharvest Biol. Technol. 9, 151–163.
Chapra, S.C., Canale, R.P., 1998. Numerical Methods for Engineers with Programming and Software Applications, third ed. WCB/McGraw-Hill, New York.
Cohen, D.S., White Jr., A.B., 1991. Sharp fronts due to diffusion and viscoelastic relaxation in polymers. SIAM J. Appl. Math. 51, 472–483.
De'Nobili, M.D., Perez, C.D., Navarro, D.A., Stortz, C.A., Rojas, A.M., 2011. Hydrolytic stability of L-(+)-ascorbic acid in low methoxyl pectin films with potential antioxidant activity at food interfaces. Food Bioprocess Technol. 6, 186–197.
De'Nobili, M.D., Curto, L.M., Delfino, J.M., Soria, M., Fissore, E.N., Rojas, A.M., 2013. Performance of alginate films for retention of L-(+)-ascorbic acid. Int. J. Pharm. 450, 95–103.
De'Nobili, M.D., Rojas, A.M., Abrami, M., Lapasin, R., Grassi, M., 2015. Structure characterization by means of rheological and NMR experiments as a first necessary approach to study the L-(+)-ascorbic acid diffusion from pectin and pectin/alginate films to agar hydrogels that mimic food materials. J. Food Eng. 165, 82–92.
Edwards, D.A., Cohen, D.S., 1995. A mathematical model for a dissolving polymer. AIChE J. 41, 2345–2355.
Favetto, G., Resnik, S., Chirife, J., Ferro Fontán, C., 1983. Statistical evaluation of water activity measurements obtained with the Vaisala Humicap humidity meter. J. Food Sci. 48, 534–538.
Ferreira, J.A., Grassi, M., Gudino, E., De Oliveira, P., 2014. A 3D model for mechanistic control of drug release. SIAM J. Appl. Math. 74, 620–633.
Ferreira, J.A., Grassi, M., Gudino, E., De Oliveira, P., 2015. A new look to non-Fickian diffusion. Appl. Math. Model. 39, 194–204.
Flory, P.J., 1953. Principles of Polymer Chemistry. Cornell University Press, Ithaca USA.
Grassi, G., Marini, J.C., 1996. Ribozymes: structure, function and potential therapy for dominant genetic disorders. Ann. Med. 28 (6), 499–510.
Grassi, G., Dawson, P., Kandolf, R., Guarnieri, G., Grassi, M., 2004. Therapeutic potential of hammerhead ribozymes in the treatment of hyper-proliferative diseases. Curr. Pharmaceut. Biotechnol. 5 (4), 369–386.
Grassi, M., Grassi, G., Lapasin, R., Colombo, I., 2007. Understanding Drug Release and Absorption Mechanisms: a Physical and Mathematical Approach. CRC Press, Boca Raton, FL, USA, pp. 1–627.
Grassi, M., Cavallaro, G., Scirè, S., Scaggiante, B., Dapas, B., Farra, R., Baiz, D., Giansante, C., Guarnieri, G., Perin, D., Grassi, G., 2010. Current strategies to improve the efficacy and the delivery of nucleic acid based drugs. Curr. Signal Transduct. Ther. 5 (2), 92–120.
Greenspan, L., 1977. Humidity fixed points of binary saturated aqueous solutions. J. Res. Natl. Bureau Standards Sect. A-Phys. Chem. 81 A (1), 89–96.
Lapasin, R., Pricl, S., 1995. Rheology of Industrial Polysaccharides. Theory and Applications. Blackie Academic and Professional, Chapman and Hall, Glasgow G64 2NZ, UK. Wester Cleddens Road, Bishopbriggs.
Lee, J.Y., Park, H.J., Lee, C.Y., Choi, W.Y., 2003. Extending shelf-life of minimally processed apples with edible coatings and anti-browning agents. Lebensm-Wiss Technol. 36, 323–329.
León, P.G., Rojas, A.M., 2007. Gellan gum films as carriers of L-(+)-ascorbic acid. Food Res. Int. 40, 565–575.
Levich, V.G., 1962. Physicochemical Hydrodynamics. Prentice-Hall.
Martín-Belloso, O., Rojas-Gräu, M.A., Soliva-Fortuny, R., 2009. Delivery of flavor and active ingredients using edible films and coatings. In: Huber, K.C., Embuscado, M.E. (Eds.), Edible Films and Coatings for Food Applications. Springer New York, New York, pp. 295–313.
Miková, K., 2001. The regulation of antioxidants in food. In: Pokorny, J., Yanishlieva, N., Gordon, M. (Eds.), Antioxidants in Foods. Practical Applications, (Chapter 11). CRC Press. Woodhead Publishing Limited, Cambridge, England, pp. 267–283.
Patankar, S.V., 1990. Numerical Heat Transfer and Fluid Flow. McGraw-Hill/Hemi-Hemisphere Publishing Corporation, New York.
Pérez, S., Mazeau, K., Hervé du Penhoat, C., 2000. The three-dimensional structures of the pectic polysaccharides. Plant Physiol. Biochem 38 (1/2), 37–55.
Perez-Gago, M.B., Serra, M., del Rio, M.A., 2006. Color change of fresh-cut apples coated with whey protein concentrate-based edible coatings. Postharvest Biol. Technol. 39, 84–92.
Rojas-Graü, M.A., Tapia, M.S., Rodríguez, F.J., Carmona, A.J., Martín-Belloso, O., 2007. Alginate and gellan based edible coatings as support of antibrowning agents applied on fresh-cut Fuji apple. Food Hydrocolloids 21, 118–127.
Shalmashi, A., Eliassi, A., 2008. Solubility of L-(+)-ascorbic acid in water, ethanol, methanol, propan-2-ol, acetone, acetonitrile, ethyl acetate, and tetrahydrofuran from (293-393) K. J. Chem. Eng. Data 53, 1332–1334.
Shi, H., 2001. Introducing natural antioxidants. In: Pokorny, J., Yanishlieva, N., Gordon, M. (Eds.), Antioxidants in Foods. Practical Applications, (Chapter 8). CRC Press. Woodhead Publishing Limited, Cambridge, England, pp. 147–155.
Swaminathan, S., Edwards, D.A., 2004. Traveling waves for anomalous diffusion in polymers. Appl. Math. Lett. 17, 7–12.
Tapia, M.S., Rodríguez, F.J., Rojas-Graü, M.A., Martín-Belloso, O., 2005. Formulation of alginate and gellan based edible coatings with antioxidants for fresh-cut apple and papaya. In: IFT Annual Meeting. New Orleans, LA. Paper 36E–43.
Truskey, G.A., Yuan, F., Katz, D.F., 2004. Transport Phenomena in Biological Systems. Pearson Prentice Hall, Upper Saddle River, New Jersey, USA.
Vincken, J.P., Schols, H.A., Oomen, R.J.F.J., McCann, M.C., Ulvskov, P., Voragen, A.G.J., Visser, R.G.F., 2003. If homogalacturonan were a side chain of rhamnogalacturonan I. Implications for cell wall architecture. Plant Physiol. 132 (4), 1781–1789.
Voragen, A.G.J., Coenen, G.J., Verhoef, R.P., Schols, H.A., 2009. Pectin, a versatile polysaccharide present in plant cell walls. Struct. Chem. 20, 263–275.
Willats, W.G.T., Knox, J.P., Mikkelsen, D., 2006. Pectin: new insights into an old polymer are starting to gel. Trends Food Sci. Technol. 17, 97–104.
Wong, W.S., Tillin, S.J., Hudson, J.S., Pavlath, A.E., 1994. Gas exchange in cut apples with bilayer coatings. J. Agric. Food Chem. 42, 2278–2285.